Article ID: 1003 - 6326(2004)05 - 0973 - 04

ZnO nanoneedles fabricated by a simple approach and their optical properties①

LU Qing-feng(路庆凤)[1], WEI Hong-xiang(魏红祥)[1, 2], HU Zhu-dong(胡柱东)[2]
(1. College of Physics & Information Engineering, Henan Normal University, Xinxiang 453007, China;
2. Institute of Physics, Chinese Academy of Sciences, Beijing 100080, China)

Abstract: Spoke-like ZnO nanoneedles have been successfully synthesized at the ambient pressure through thermally oxidizing Zn powders containing Au nanoparticles. X-ray diffraction analysis indicates that the ZnO nanoneedles have a hexagonal wurtzite structure of the crystalline ZnO. The morphology of the products was examined by FE-SEM. The photoluminescence(PL) spectrum under 325 nm exhibits both an UV emission and a green emission. It is interesting to note that the heating rate plays a key role in the synthesis of ZnO nanoneedles. Based on this discovery we propose to explain the special growth behavior as novel mechanism that a large temperature gradient and Au nanoparticles simultaneously result in the spoke-like ZnO nanoneedles growth.

Key words: ZnO nanoneedles; photoluminescence spectrum; optical properties
CLC number: Q 482.31 **Document code:** A

1 INTRODUCTION

Over the past few years great efforts have been invested to synthesize various wide band-gap semiconductor materials such as CdS[1], GaN[2, 3], ZnO[4] and InP[5] because of the ever-increasing commercial desire for short wavelength light emitting devices and ultrafast nonlinear optical devices. ZnO, a wide band-gap (3.37 eV) compound semiconductor, exhibits the strong exciton binding energy (about 60 meV) which is substantially larger than its thermal energy (26 meV) at room temperature and that of ZnSe (22 meV) and GaN (25 meV)[6-8]. The high exciton binding energy can ensure an efficient excitonic laser action in ZnO crystal at room temperature under low excitation intensity. In addition, ZnO has high mechanical and thermal stability. Consequently, ZnO is recognized as a promising candidate for blue optoelectronic applications. Most of the studies performed on ZnO were focused on the disordered particles and thin films. Recently large scale synthesis of one dimensional (1D) ZnO with various morphologies has been achieved, such as nanowires[9-13], nanorods[14-18], nanonails[19], nanoneedles[20] and nanobelts[21]. Because low-dimensionality of ZnO can further lower the threshold in which quantum size effects yield a substantial density of states at the band edges and enhance radiative recombination due to carrier confinement.

So far a large variety of methods, such as MOVPE[22, 23], anodic alumina membrane templates[10, 24-26], microemulsion hydrothermal process[13], reduction and oxidation of ZnS[27], and vapor transport[28-30], have been developed for the fabrication of nanostructure ZnO. In most of the means, however, complex gas system and vacuum system are required. Moreover, the growth mechanism of nanostructure ZnO with different shapes is not so clear. Therefore it is necessary to obtain a mild approach to produce high-purity nanostructure ZnO with a high yield at low cost. Simultaneously it is of great significance to probe the growth mechanism. Herein, a simple thermal oxidation route employed to synthesize ZnO nanoneedles is reported and the growth mechanism is discussed.

2 EXPERIMENTAL

ZnO nanoneedles were produced via thermally oxidizing commercial Zn (AR grade) powders containing Au nanoparticles in the atmosphere and no carrier gas was needed. The details of the experimental procedure have been described elsewhere[29]. Briefly, the Au nanoparticles were obtained through a reaction of gold salt with sodium citrate. Sodium citrate (60 mg) in 100 mL water was boiled for 15 min and 1 mL of aqueous solution containing 9.5 mg $HAuCl_4$ was added. And then some Zn powders were immersed in the solution containing Au nanoparticles for about 20 - 24 h and then dried at room temperature and ground into powders. After that, the as-prepared Zn powders were placed in a quartz boat. Subsequently, the quartz boat has been placed at the cen-

① **Foundation item:** Project(10274103) supported by the National Natural Science Foundation of China
Received date: 2004 - 01 - 05; **Accepted date:** 2004 - 05 - 27
Correspondence: LU Qing-feng, Professor, PhD; Tel: +86-10-82648063; E-mail: hxwei@aphy.iphy.ac.cn

ter of a quartz tube that was introduced into a horizontal tube furnace. With both ends of the quartz tube open to the atmosphere, the furnace was rapidly heated to 550 ℃. When the temperature was raised up to about 500 ℃, an expanding yellow flame bulb burned up around the Zn powders and heating was held until the flame bulb died away. Then the furnace cooled down to room temperature. At a high heating speed, the white fluffy products were found in the quartz boat.

The morphologies of the as-synthesized products were characterized using a Hitachi S-4200 field emission scanning electron microscope (FE-SEM). X-ray diffraction measurement was taken on a Rigaku D/MaX-2400 X-ray diffractometer with CuK_α radiation. Raman spectroscopy was obtained using a SPEX-1403 spectrometry system from 100 to 900 cm^{-1} at room temperature. The 488 nm line of an Ar^+ laser was used for excitation, with the capability of supplying 40 mW. The PL measurements were carried out on a Hitachi 850 VIS-UV spectrophotometer with a Xe lamp focused in about 0.1 mm as the excitation light source at room temperature. The excited wavelength was 325 nm and a 345 nm filter was used.

3 RESULTS AND DISCUSSION

X-ray diffraction (XRD) pattern was taken to examine the crystal structure of the products. Bulk quantity of the samples was analyzed by XRD. Fig. 1 shows a typical XRD pattern of the as-produced ZnO. The diffraction peaks can be well indexed to a hexagonal structure of the crystalline ZnO with cell constants of a= 3.249 Å and c= 5.206 Å (JCPDS card no. 36-1451). No diffraction peaks from Zn and Au were detected. In an oxygen-rich environment, all Zn easily transforms to ZnO. Au was not detected because the initial Au content is little and it is partially solved in the ZnO. The strong intensity of ZnO diffraction peaks reveals that the resulting products are ZnO wurtzite phase with high purity.

Fig. 2(a) shows the general morphology of as-prepared ZnO at a heating rate of 160 ℃/min. The image clearly shows the formation of spoke-like ZnO nanoneedles. It is noted that impurities are not observed. Careful examination of individual nanoneedle indicates that the diameters of the nanoneedles range from 15 to 120 nm and their lengths are up to several tens of micrometers. The high magnification view is shown in Fig. 2(b). It is interesting to observe a hexagon-shaped pyramid-like nanoneedle at the root of as-grown ZnO nanoneedles. The terraced-shape suggests that the growth of ZnO nanoneedles can not be explained

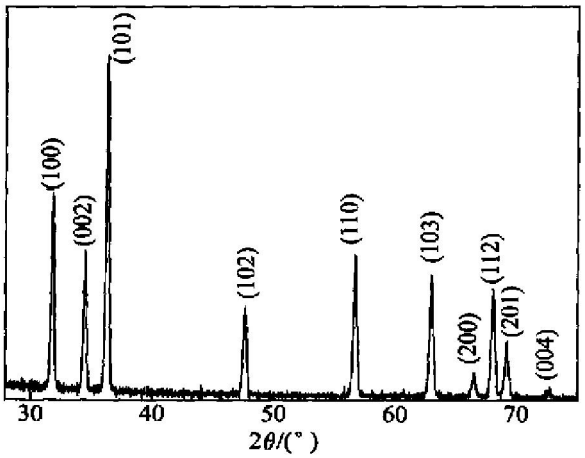

Fig. 1 XRD pattern of ZnO nanoneedles

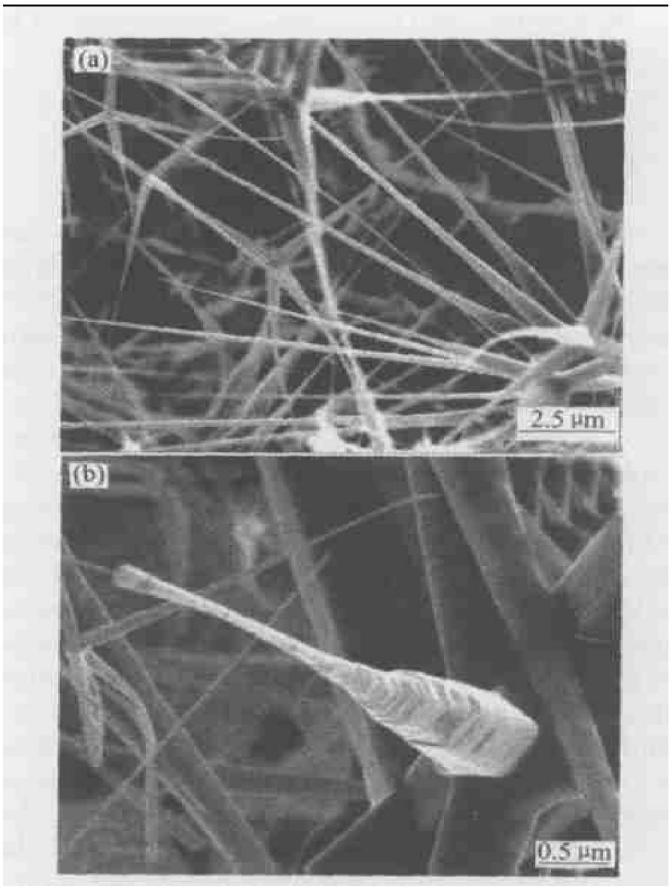

Fig. 2 FE-SEM images of ZnO nanoneedles
(a) —Large magnification; (b) —Low magnification

using classical catalyst-assisted VLS mechanism. In the known VLS mechanism, the metal nanoparticles play a critical role in growing nanowires. The size of individual nanowire or nanotube depends on that of metal catalyst clusters. As for a single tube or wire, the diameter fluctuation of both ends is negligible. In this case, however, the diameter gradually tapers off from the root to the tip. The similar steps at the tip of ZnO nanoneedles were observed by other authors[23]. This surprising behavior stimulates us to carry out the preparation of ZnO in the absence of Au nanoparticles under the same condition. Only small

amount of nanowiskers were observed in this case. Spontaneously, we are convinced that the nanosized gold particles play a novel role rather than the catalyst in forming liquid droplets that absorb gas reactants.

From the SEM images, a novel growth mechanism different from classic VLS mechanism was proposed to explain the formation of ZnO nanoneedles. When we rapidly heat the Zn powders to 500 ℃, which is well above melting point (419 ℃) of Zn but below that of gold (961 ℃), the Zn powders melt while the gold nanoparticles still remain solid. The active Zn vapor in the surface of Zn liquid with gold nanoparticles embedded reacts with oxygen around. The Au nanoparticles work as nuclei. The Zn vapor reacts with oxygen directly and adheres to the front of the nanoneedles, instead of reacting with Au nanoparticles first and then transforms to ZnO. The heat generated from the reaction of Zn and O_2 leads to a temperature gradient, which results in radial growth. Meanwhile, the crystal ZnO nanoneedles form. In this case, there is only free convection in the quartz tube and the thermal transport is inefficient. The buoyancy force from a temperature gradient may bring about radial mass transport, which accounts for the yellow flame bulb observed during the growth of ZnO nanoneedles. Thus the temperature decreases over the Zn liquid spokewise, which promotes the radical growth of ZnO nanoneedles. With the development of ZnO, the Zn vapor and the oxygen are consumed simultaneously and the free convection limits the transport of Zn and oxygen. Therefore the ZnO nanoneedles taper off, as shown in Fig. 2(a). The temperature fluctuation also can influence the variation of the growth rate. Fig. 2(b) results from a combination of a temperature gradient and concentration fluctuation of Zn and oxygen. When Zn powders are depleted forming into ZnO nanoneedles, the growth terminates.

ZnO nanoneedles were not observed but ZnO nanosheets and ZnO in other hybrid shape were found when the heating rate was below 150 ℃/min or lower, though the heating temperature was raised up to 1 000 ℃. Low heating speed corresponds to small temperature gradient, i. e. weak drive for growing. It further suggests that the large temperature gradient is the main drive force of radial growth of ZnO nanoneedles.

Raman spectrum of as-synthesized ZnO nanoneedles is illustrated in Fig. 3. ZnO has wurtzite symmetry with C_{6v} or 6 mm symmetry. There are four atoms per unit cell leading to 12 phonon branches, nine optical and three acoustic. As shown in Fig. 3, the peak at 438 cm^{-1} is attributed to ZnO nonpolar optical phonons E_2 mode, which is typical of one of Raman active branches. In contrast, the peaks at 328 cm^{-1} and 584 cm^{-1} are very weak. Obviously, it further demonstrates that the products are composed of ZnO with hexagonal structure.

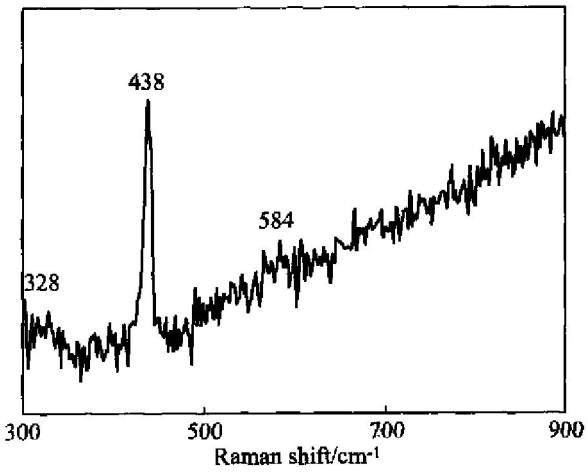

Fig. 3 Raman spectrum acquired from as-prepared ZnO nanoneedles

The PL measurement of ZnO nanoneedles were taken on the bulk amount of the products at room temperature. Fig. 4 shows the PL spectrum of as-made ZnO nanoneedles. A narrow UV peak centered at 3.22 eV (about 386.1 nm in wavelength) and a broad green peak at 2.47 eV (about 503.2 nm in wavelength) were detected in the PL spectrum at low excitation intensity (5.5 mW). Whilst the UV emission corresponds to the near band-edge transition, namely the recombination of free excitons through an exciton-exciton collision process, and the green emission peak is commonly referred to a deep-level or trap-state emission. The appearance of UV band emission with low excitation intensity at room temperature is attributed to the radial quantum confinement effect of ZnOnanoneedles. The green band emission results

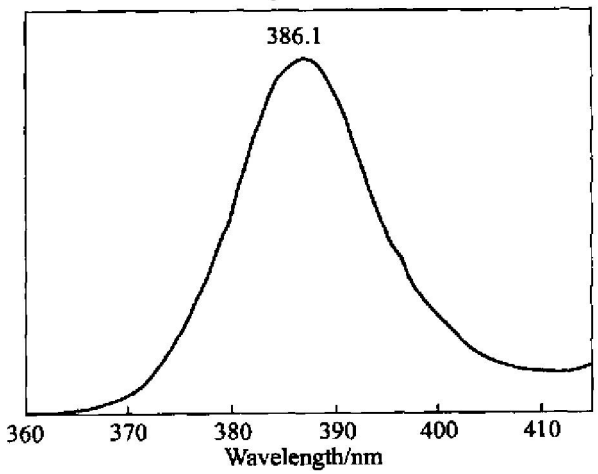

Fig. 4 PL spectrum of ZnO nanoneedles measured at room temperature

from the radial recombination of a photo-generated hole with an electron that belongs to a singly ionized oxygen vacancy.

REFERENCES

[1] DUAN X F, HUANG Y, Agarwal R, et al. Single-nanowire electrically driven lasers[J], 2003, 421: 241-245.

[2] HAN W Q, FAN S S, LI Q Q, et al. Synthesis of gallium nitride nanorods through a carbon nanotube-confined reaction[J]. Science, 1997, 277: 1287-1289.

[3] Johnson J C, Choi H J, Knutsen K P, et al. Single gallium nitrid nanowire lasers[J]. Nature Materials, 2002, 1: 106-110.

[4] Bagnall D M, CHEN Y F, ZHU Z, et al. Optically pumped lasing of ZnO at room temperature[J]. Appl Phys Lett, 1997, 70: 2230-2232.

[5] DUAN X F, HUANG Y, CUI Y, et al. Indium phosphide nanowires as building blocks for nanoscale electronic and optoelectronic devices[J]. Nature, 2001, 409: 66-69.

[6] White A E, Short K T, Dynes R C, et al. Mesotaxy: single-crystal growth of buried $CoSi_2$ layers[J]. Appl Phys Lett, 1987, 50: 95-97.

[7] Service R F. Materials science: will UV lasers beat the blues? [J]. Science, 1997, 276: 895-896.

[8] DAI Ying, ZHANG Yue, BAI Yuan-qiang, et al. Bicrystalline zinc oxide nanowires[J]. Chem Phys Lett, 2003, 375: 96-101.

[9] Lyu S C, ZHANG Y, Ruh H, et al. Low temperature growth and photoluminescence of well-aligned zinc oxide nanowires[J]. Chem Phys Lett, 2002, 363: 134-138.

[10] LI Y, MENG G W, ZHANG L D, et al. Ordered semiconductor ZnO nanowire arrays and their photoluminescence properties[J]. Appl Phys Lett, 2000, 76: 2011-2013.

[11] DONG L F, JIAO J, Tuggle D W, et al. ZnO nanowires formed on tungsten substrates and their electron field emission properties[J]. Appl Phys Lett, 2003, 82: 1096-1098.

[12] Kim H, Sigmund W. Zinc oxide nanowires on carbon nanotubes[J]. Appl Phys Lett, 2002, 81: 2085-2087.

[13] ZHANG J, SUN L D, PAN H Y, et al. ZnO nanowires fabricated by a convenient route[J]. New J Chem, 2002, 26: 33-34.

[14] XU C K, XU G D, LIU Y K, et al. A simple and novel route for the preparation of ZnO nanorods[J]. Solid State Commun, 2002, 122: 175-179.

[15] GUO L, JI Y L, XU H B, et al. Regularly shaped, single-crystalline ZnO nanorods with wurtzite structure [J]. J Am Chem Soc, 2002, 124: 14864-14865.

[16] Iwanaga H, Fujii M, Ichihara M, et al. Some evidence for the octa-twin model of tetrapod ZnO particles[J]. J Cryst Growth, 1994, 141: 234-238.

[17] Kitano M, Hamabe T, Maeda S. Growth of large tetrapod-like ZnO crystals: experimental considerations on kinetics of growth[J]. J Cryst Growth, 1990, 102: 965-973.

[18] DAI Y, ZHANG Y, LI Q K, et al. Synthesis and optical properties of tetrapod-like zinc oxide nanorods[J]. Chem Phys Lett, 2002, 358: 83-86.

[19] LAO J Y, HUANG J Y, WANG D Z, et al. ZnO nanobridges and nanonails[J]. Nanoletters, 2003, 3: 235-238.

[20] Park J W I, Gyu-Chul Y, Kim W. Schottky nanocontacts on ZnO nanorod arrays[J]. Appl Phys Lett, 2003, 82: 4358-4360.

[21] LI Y B, Bando Y, Sato T, et al. ZnO nanobelts grown on Si substrate[J]. Appl Phys Lett, 2002, 81: 144-146.

[22] Kirchner C, Gruber Th, Reuβ F, et al. MOVPE growth of ZnO using various oxygen precursors[J]. J Cryst Growth, 2003, 248: 20-24.

[23] Park W I, Kim D H, Jung S W, et al. Metalorganic vapor-phase epotaxial growth of vertically well-aligned Zn nanorods[J]. Appl Phys Lett, 2002, 80: 4232-4234.

[24] LI Y, MENG G S, ZHANG L D. Fabrication of highly ordered ZnO nanowire arrays in anodic alumina membranes[J]. J Mater Res, 2000, 15: 2305-2308.

[25] Wang Y C, Leu I C, Hon M H. Preparation and characterization of nanosized ZnO arrays by electrophoretic deposition[J]. J Cryst Growth, 2002, 237-239: 564-568.

[26] Vayssieres L, Keis K, Lindquist S E, et al. Purpose-built anisotropic metal oxide material: 3D highly oriented microrod array of ZnO[J]. J Phys Chem B, 2001, 105: 3350-3352.

[27] YUAN H J, XIE S S, LIU D F, et al. Characterization of zinc oxide crystal nanowires grown by thermal evaporation of ZnS powders[J]. Chem Phys Lett, 2003, 371: 337-341.

[28] ZHAO Q X, Willander M, Morjan R E, et al. Optical recombination of ZnO nanowires grown on sapphire and Si substrates[J]. Appl Phys Lett, 2003, 83: 165-167.

[29] WANG Y W, ZHANG L D, WANG G Z, et al. Catalytic growth of semiconducting zinc oxide nanowires and their photoluminescence properties[J]. J Cryst Growth, 2002, 234: 171-175.

[30] KONG Y C, YU D P, ZHANG B, et al. Ultraviolet-emitting ZnO nanowires synthesized by a physical vapor deposited approach[J]. Appl Phys Lett, 2001, 78: 407-409.

(Edited by YANG Bing)